International Journal of Pharmaceutics 548 (2018) 454–465

Contents lists available at ScienceDirect

International Journal of Pharmaceutics

journal homepage: www.elsevier.com/locate/ijpharm

Improvement of cutaneous delivery of methylene blue by liquid crystals

Maria Teresa Junqueira Garcia[a,*], Thalita Pedralino Gonçalves[a], Éricka São Félix Martins[a], Tereza Silva Martins[a], Márcia Carvalho de Abreu Fantini[b], Paulo Roberto Regazi Minarini[a], Sandra Costa Fernandez[c], Giovanna Cassone Salata[c], Luciana Biagini Lopes[c]

[a] Instituto de Ciências Ambientais, Químicas e Farmacêuticas, Universidade Federal de São Paulo, Rua: São Nicolau 210, Diadema, SP, Brazil
[b] Instituto de Física, Universidade de São Paulo, Rua do Matão 1371, São Paulo, SP, Brazil
[c] Instituto de Ciências Biomédicas, Universidade de São Paulo, Av. Prof. Lineu Prestes 1524, São Paulo, SP, Brazil

ARTICLE INFO

Keywords:
Brij 97®
Lamellar phase
Hexagonal phase
Methylene blue
Photodynamic therapy
Skin delivery

ABSTRACT

The purpose of this study was to evaluate the effect of composition and characteristics of liquid crystalline phases (LCPs) on cutaneous delivery of methylene blue (MB). LCPs were obtained by mixing Brij97® with water at various ratios; Brij97®:water at 8:2 (F8:2), 7:3 (F7:3), and 6:4 (F6:4) were selected, and MB was incorporated at 0.1%. F8:2 and F7:3 exhibited textures and small angle X-ray scattering (SAXS) patterns corresponding to lamellar phase, whereas F6:4 displayed characteristics of hexagonal phase. All three LCPs were stable for 9 months, and exhibited thixotropic pseudoplastic behaviour. Increasing water content increased viscosity. All three LCPs released less (3.2- to 6.6-fold) MB than control gel (3.0% hydroxyethylcellulose (HEC) + 0.1% MB), demonstrating their ability to sustain release. Despite the lower release, all LCPs improved skin retention of MB at 6 h post-application (1.3- to 2.1-fold) compared to the control gel. Among the LCPs, F8:2-mediated skin retention of MB was more pronounced, followed by F7:3. Consistent with the increased penetration, transepidermal water loss (TEWL) also increased after treatment with the LCPs (2.0–2.8 fold), which suggests their influence on skin barrier. Irritation studies by Hen's Egg Test – Chorioallantoic Membrane (HET-CAM) suggest that F7:3 and F6:4 may be better tolerated by the skin than F8:2.

1. Introduction

Methylene Blue (MB) is a cationic chromophore from the phenothiazine family that exhibits adequate photophysical and photochemical properties as photosensitizer (FTS) for photodynamic therapy (PDT), which include intense absorption in the 550–700 nm region and considerable quantum yield of singlet oxygen (Tardivo et al., 2005). In addition, it has low toxicity, can be easily obtained on an industrial scale with good reproducibility and low cost and the irradiation source for its excitation can be obtained at low cost (Tardivo et al., 2005). MB induces phototoxic effects in a variety of tumor cells (Guan et al., 2014; Seong and Kim, 2015; Tardivo et al., 2005; Yu et al., 2014), including skin cancer cells (Samy et al., 2015).

Cutaneous delivery of MB is an interesting strategy to provide therapeutic effect to a specific site with reduced systemic toxicity. So far, MB has been administrated mostly by intralesional injection for an adequate therapeutic response (Baran et al., 2010; Orth et al., 2000, 1998; Tardivo et al., 2005, 2004). The need for intralesional injection of MB is justified by the drug physicochemical properties; as a hydrophilic drug with a low octanol/water partition coefficient (Log $P = -0.9$) (Walker et al., 2004), its partition and diffusion through the stratum corneum, the outermost layer of the skin, is limited, preventing it from reaching cutaneous deeper layers at adequate concentrations. This is further supported by results from a recent study in which topical application of MB in liposomal vesicles, associated or not with intralesional injection of MB, was successful after superficial curettage of cutaneous tumor lesions (Samy et al., 2015), demonstrating the need of mechanical removal of part of the injured tissue to allow penetration of MB at a sufficient quantity to optimize PDT results. Thus, strategies to improve cutaneous delivery of MB are clearly needed.

In face of these facts, we proposed the development of topical systems capable of enhancing cutaneous penetration of MB for PDT and treatment of neoplastic cutaneous lesions. Polyoxyethylene (10) oleyl ether (Brij 97®) is a nonionic surfactant derived from ethylene oxide widely used for the development of drug delivery systems (Hosmer et al., 2011; Pepe et al., 2013; Phelps et al., 2011; Rissi et al., 2014). When dispersed in water at a concentration higher than the critical micellar concentration (CMC), Brij 97® self-aggregates, resulting in

* Corresponding author.
E-mail address: mtjgarcia@unifesp.br (M.T. Junqueira Garcia).

https://doi.org/10.1016/j.ijpharm.2018.07.003
Received 25 March 2018; Received in revised form 28 June 2018; Accepted 1 July 2018
Available online 02 July 2018

various types of liquid crystalline structures of interest for cutaneous delivery of drug (Hosmer et al., 2013, 2011). These phases can be easily prepared and display adequate consistency for topical use. Moreover, Brij series surfactants act as absorption enhancer, increasing the permeability of biological membranes like the skin (Hosmer et al., 2011; Park et al., 2000).

The aim of this study was to evaluate the effect of water content and internal structure of liquid crystals based on Brij97® on cutaneous delivery of MB. For this purpose, liquid crystalline phases based on Brij97® were obtained, identified by polarized light microscopy and small angle X-ray scattering, and characterized regarding to stability, rheological behaviour and MB release profile. In addition, the effect of liquid crystalline phases on the barrier function of the skin and on *in vitro* cutaneous delivery of MB was evaluated. To complement the study, the irritation potential of liquid crystalline phases was carried out using Hen's Egg Test – Chorioallantoic Membrane (HET-CAM). Although the effect of topical administration of MB for PDT has been carried out *in vivo* (Fadel and Tawfik, 2014; Moftah et al., 2016; Samy et al., 2015; Tardivo et al., 2005), to the best of your knowledge, our study is the first aiming to assess the influence of formulation composition on MB skin localization.

2. Material and methods

2.1. Material

Brij 97® (polyoxyethylene 10 oleyl ether) was kindly supplied by Croda do Brasil Ltda (Campinas, São Paulo, Brazil). Methylene blue and potassium phosphate monobasic (KH_2PO_4) were of analytical grade and were purchased from Synth (Diadema, São Paulo, Brazil). Hydroxyethylcellulose was of pharmaceutical grade and was purchased from Mapric (São Paulo, São Paulo, Brazil). Reverse Osmosis system (Veolia, Brasil) was used to purify the water used.

2.2. Methods

2.2.1. Obtaining liquid-crystalline systems

The systems were obtained by mixing Brij 97® with water in ratios varying from 9:1 to 1:9 (w/w) in a vortex for 5 min, at room temperature. MB was previously dissolved in the water, resulting in a mixture at a final concentration of 0.1% (w/w). The systems were packed in glass bottles, closed and allowed to equilibrate for 7 days before use at room temperature and protected from light, as MB is a photosensitive drug (the bottles were wrapped in aluminum foil and stored in light-protected environments). To evaluate the influence of the liquid crystalline phases on the cutaneous penetration of MB, three systems containing Brij97®:water at 8:2 (w/w, F8:2), 7:3 (w/w, F7:3), and 6:4 (w/w, F6:4) were selected. These proportions were chosen for two reasons: first, the content of 20%–60% of water is necessary for liquid crystalline phase formation; and second, the consistency should be appropriated for topical application, being more viscous than fluid isotropic dispersions, but not too stiff and difficult to spread. A 3.0% (w/w) hydroxyethylcellulose (HEC) gel containing 0.1% (w/w) of MB was used as control formulation. This gel was selected for three reasons: first, the HEC polymer is a nonionic water soluble polymer; second, at a final concentration of 3.0% (w/w), the gel has appropriate consistency for topical use; and third, considering that formulation viscosity may interfere on drug release and penetration, we opted for using a control formulation with viscosity close to the less viscous formulation (F8:2). The HEC gel was obtained by previously dispersion of polymer in sufficient quantity of water; MB was solubilized in the remaining water and incorporated into the dispersion, resulting in a mixture at a final concentration of 0.1% (w/w). The systems were packed in glass bottles, closed and allowed to equilibrate for 7 days before use at room temperature and protected from light (the bottles were wrapped in aluminum foil and stored in light-protected environments).

2.2.2. Polarized light microscopy

Considering that some liquid crystals are birefringent, the type of liquid crystalline structure was identified under a polarized light microscope (Carl Zeiss, Axio Imager A2, Germany), equipped with an AxioCam MRc camera and AxioVision software (Carl Zeiss, Germany). The lamellar phase texture is characterized by a woven structure and/or a mosaic or maltese cross pattern, while the hexagonal phase exhibits non-geometric and fan-like texture (Ganem-Quintanar et al., 2000). Fluid isotropic dispersions and aqueous phase containing surfactant aggregates are non-birefringent and only a black background with no well-characterized texture is displayed. For identification, a small amount of the formulation was placed on a glass slide and covered with a coverslip, and analyzed by a polarized light microscope at room temperature. A phase diagram was constructed to show the relationship between composition and phase behaviour of the samples.

2.2.3. Small angle X-ray scattering (SAXS) analysis

SAXS analyses were carried out to identify the liquid crystalline structure and evaluate the influence of the addition of MB at various concentrations (0.1% and 0.2%, w/w). The measurements were obtained with the NANOSTAR (Bruker) equipped with a sealed copper tube (Cu-Kα, $\lambda = 1.5418\,Å^{-1}$) operating at 40 kV and 30 mA. The collimation system was composed of Göbel mirrors and the point focus geometry was used. The samples were placed between two thin polyimide film foils (Kapton®) in the sample holder and kept under vacuum at a pressure of approximately 10^{-2} Torr. A sample-detector distance of 67 cm was set, resulting in scattering vectors $q = ((4\pi\sin\theta)/\lambda)$ values ranging from $0.012\,Å^{-1}$ to $0.35\,Å^{-1}$. The acquisition time was 20 min. All data were normalized by the measuring time and were corrected for the absorption effects.

2.2.4. Rheology

The rheological behaviour is an important property to be considered in the development of drug delivery systems because of its relationship with the structural organization and interaction among components, which can influence the formulation applicability and drug release profile. The rheological behaviour of the selected liquid crystalline phases was determined using cone and plate rheometer (RST-CPS Cone/Plate, Brookfield, Middleboro, MA) equipped with Rheo3000 software. The experiments were performed with the progressive increase and decrease of shear rates (range of 0–80 s^{-1}) at room temperature. Each stage lasted 120 s. The relationship between shear rate and shear stress, as well as between shear rate and viscosity were graphically obtained; 3.0% (w/w) hydroxyethylcellulose (HEC) gel containing 0.1% (w/w) of MB was used as control formulation. The rheogram data were evaluated using Power law equation:

$$\tau = K\gamma^n \quad (1)$$

where τ = shear stress, γ = shear rate, K = consistency index and n = flow index (Mahdi et al., 2011).

2.2.5. Stability study

F8:2, F7:3 and F6:4 were stored at room temperature (25 °C) for 9.0 months and protected from light (the bottles were wrapped in aluminum foil and stored in protected light environments). At pre-determined intervals (1.5, 4.0, 6.0 and 9.0 months), the samples were observed under a polarized light microscope to evaluate changes on the liquid crystalline structure, and MB content was assessed by spectrophotometry (Thermo Scientific, Madison, WI) at 662 nm after dilution with water. Three samples of each formulation were prepared and analyzed throughout the 9 months period (n = 3).

2.2.6. Quantification of MB

The methodology employed for the quantification of MB was UV/Vis Spectrophotometry (Thermo Scientific, Madison, WI) (Junqueira et al., 2016) at 662 nm. Standard curves of MB (2.5–20 μg/mL) were

prepared in phosphate buffer (pH7.2, 0.1 M). The method was linear at the selected concentration range (r = 0.999) and the coefficients of inter- and intra-assay variation and accuracy were within the permitted range for the method (≤5%) (Brasil, 2003), indicating good reproducibility and accuracy. The detection and quantification limit values were obtained from the curve parameters, and were 0.199 μg/mL and 0.665 μg/mL, respectively.

2.2.7. In vitro release of MB

Considering that the difference in the topical delivery of drugs may result from the difference in drug release, *in vitro* MB release studies were carried out. MB release profile from liquid crystalline phases was performed using cell culture inserts (Hosmer et al., 2013, 2011) with polyethylene terephthalate membrane of 1 μm pores (Becton Dickinson, France, area of 0.785 cm^2), as support for 250 mg of the formulation (donor compartment) and 5.0% (w/w) hydroxyethylcellulose (HEC) gel (2.0 g) used as receptor phase. The HEC in the receptor compartment was employed because it may simulate better the diffusion condition of the skin and minimize or delay phase transition during the experiment, which is commonly associated with the migration of solvent from the receptor compartment (Hosmer et al., 2013; 2011). After 1, 2, 3, 4, 5 and 6 h from the beginning of the release studies, the gel of the receptor compartment was removed, diluted in 0.1 M phosphate buffer (pH7.2), and MB quantified by spectrophotometry. The procedure was standardized to verify the influence of 5.0% HEC on reading by spectrophotometry of MB by spiking the receptor phase gel with MB solution to obtain final drug concentrations after dilution (in 0.1 M phosphate buffer (pH7.2)) varying from 5.0 to 15.0 μg/mL and it was compared to same MB concentration in 0.1 M phosphate buffer (pH7.2). Both conditions exhibited similar results, suggesting that presence of HEC exerted no influence on drug quantification.

Images of the formulations in polarized light microscope were obtained after the 6 h from the beginning of the release studies to ensure absence of phase transitions. HEC gel (3.0%, w/w) containing 0.1% (w/w) of MB was used as control formulation.

The MB release profile was obtained by plotting the cumulative percentage of MB released from initial loading of MB versus time.

The data from the MB release studies were analyzed by employing different kinetic models: zero-order (amount released versus time), and first-order (log of the amount remaining in the system versus time).

The experiment was performed in quintuplicate or sextuplicate for each formulation.

2.2.8. In vitro skin retention of MB

Pig ears obtained from a local slaughterhouse (Raja, Carapicuíba, São Paulo) had the dorsal skin carefully dissected with a scalpel and the subcutaneous fat tissue was carefully removed using surgical scissors to obtain a full-thickness skin. The integrity of the skin was assessed by visual observation. Skin sections with any wounds, punctures, bleeding, skin disease, cuts or holes on the surface were discarded. The skin sections were stored at −20 °C for a maximum of 4 weeks before use (Hosmer et al., 2013).

For *in vitro* skin retention studies, pig ear full-thickness skin sections were mounted on adapted vertical diffusion cells (diffusion area of 3.8 cm^2), previously calibrated, with the stratum corneum facing the donor compartment, while the dermis was maintained in contact with the receptor phase (phosphate buffer pH 7.2, 0.1 M). The receptor solution (10 mL) was maintained at 37 °C under constant stirring (400 rpm); under these conditions, the temperature on the skin surface was 32 °C (Hosmer et al., 2011). The formulations (1.0*g*) were applied to the donor compartment (with a spatula) for 3 or 6 h, after which excess of the formulation was carefully removed with a spatula, skin sections were rinsed, carefully blotted dry and the penetration region (exposed to the formulation) was cut into small pieces, placed in 5 mL of phosphate buffer (pH7.2, 0.1 M), homogenized (Ultra-Turrax T18, IKA) for 1 min at ambient temperature and sonicated for 20 min for the extraction of MB. The product obtained was filtered using a 0.45 μm pore membrane and the amount of MB retained in the skin was determined by spectrophotometry. The extraction procedure was standardized by spiking the skin with MB solution to obtain final drug concentrations in homogenates varying from 2.5 to 10 μg/mL. Homogenates were prepared as previously described and MB was assayed by UV/Vis spectrophotometer. MB recovery varied from 78% to 83%. Skin homogenates, as well as Brij-based systems do not absorb at the wavelength used, so they do not interfere with MB quantification. Hydroxyethylcellulose gel (3.0%, w/w) containing 0.1% (w/w) of MB was used as control formulation.

The experiment was performed in quintuplicate or sextuplicate for each formulation.

2.2.9. In vitro transepidermal water loss (TEWL)

The TEWL was used as a parameter to measure the influence of the formulation on the barrier function of the skin. For the assay, it was used a closed chamber evaporimeter (Vapometer, Delfin Technologies Ltd., Kuopio, Finland) equipped with an adaptor to fit the diffusion cell (Hanson Research, Chatsworth, CA, diffusion area of 1.7 cm^2) opening (Thomas et al., 2014). Basal TEWL values were measured after skin equilibrium for 15 min in diffusion cells containing 0.1 M phosphate buffer (pH 7.2) in the receptor compartment. Measurements were taken for 10 s. Tissues were subsequently treated with the formulations, water and the 3.0% HEC gel were used as controls. After 6 h of exposure, the formulations were carefully removed with a spatula, skin sections were rinsed with 10 mL of purified water, and carefully blotted dry with 2 pieces of humid tissue paper and 3 pieces of dry tissue paper. To ensure that any effect of the cleaning process was taken into consideration in the results, the skin sections treated with the controls were subjected to the same cleaning procedure. The sections were subsequently replaced in the diffusion cells, and after 15 min to establish equilibrium, measurements of TEWL were carried out. Results were expressed as the difference between TEWL values after treatment (6 h) and before treatment (basal values). The experiment was performed in quadruplicate or quintuplicate for each formulation.

2.2.10. Fluorescence microscopy

Because the F8:2 lamellar phase promoted the highest drug penetration in the skin, it was selected for further studies. To evaluate whether penetration of MB from this formulation is homogenous throughout the surface of the skin, the distribution of MB was studied using fluorescence microscopy. Hydroxyethylcellulose gel (3.0%, w/w) containing 0.1% (w/w) of MB was used as control formulation.

Pig ear full-thickness skin sections were mounted on adapted vertical diffusion as previously described in the "*in vitro* skin retention of MB" section. The experimental conditions were maintained. The formulations (1.0 g) were applied in the donor compartment (F8:2 or control (HEC 3.0%, w/w) containing 0.1% (w/w) of MB). After 6 h, the formulations were carefully removed with a spatula, skin sections were rinsed, carefully blotted dry and the diffusion area of skin samples was frozen, embedded in Tissue-Tek OCT compound (Pelco International, Redding, California) and sectioned using a cryostat microtome (Leica, Wetzlar, Germany) at 10 μm. The slides were visualized without any additional staining or treatment through a 20× objective using a fluorescence microscope (Carl Zeiss, Axio Imager A2, Germany) equipped with a filter for Rhodamine, an AxioCam MRc camera and AxioVision software (Carl Zeiss, Germany).

Skin sections treated with 0.1 M phosphate buffer (pH 7.2) were used as a control to determine tissue autofluorescence. The experiment was performed in triplicate for each formulation.

2.2.11. Irritation potential

Hen's Egg Test – Chorioallantoic Membrane (HET-CAM) was used to evaluate the irritation potential of the formulations. Fertilized chicken eggs were obtained from Sabor Natural (São Paulo, SP, Brazil) and

incubated for 9 days at 37 °C and 55% humidity in incubators (Premium Ecologica, Belo Horizonte, MG, Brazil) with automatic rotation every 2 h. Following exposure and photodocumentation of the chorioallantoic membrane (Nikon, SMZ 1500, Tokyo, Japan), 100 mg of each formulation were carefully applied on the exposed membrane, and left for 300 s; NaCl 0.9% and NaOH (0.1 M) were used as negative and positive controls, respectively. All formulations were warmed to 32 °C before application to avoid vasoconstriction. Coagulation, hemorrhage and lysis were assessed at 0, 30, 60, 120, 180, 240 and 300 s following membrane exposure to the treatments. At 300 s, the formulations were carefully removed with tweezers, the membrane rinsed with saline (5 mL) and further inspected. The irritation index was calculated using the following equation as previously described (ICCVAM, 2010):

$$II = ((301-h)/300) \times 5 + ((301-l)/300) \times 7 + ((301-c)/300) \times 9 \quad (2)$$

where h, l and c are the time (in s) of the beginning of hemorrhage, lysis or coagulation. The following classification was used: II < 0.9: not labeled; 1.0 < II < 4.9: slightly irritating; 5.0 < II < 8.9: moderately irritating; 9.0 < II < 21: severely irritating (ICCVAM, 2010). Each treatment was performed in 3–5 eggs.

2.2.12. Data analysis

The results were reported as mean ± SD. Data were statistically analyzed using the One-way ANOVA test followed by Tukey Kramer post-hoc test using GraphPad Prism 5.0 software. Values were considered significantly different when $p < 0.05$.

3. Results

3.1. Polarized light microscopy

Brij97® is an amphiphilic surfactant (HLB12.4) that self-aggregates forming several types of structures in aqueous solution. The structure formed depends on the Brij97® concentration and temperature. At room temperature, and with progressive water addition, formation of isotropic micellar systems (10% water), lamellar phase (20%–30% water), hexagonal phase (40%–60% water) and aqueous phase containing surfactant aggregates (≥70% water) was observed (Fig. 1).

Three systems were selected for further studies: two lamellar phases containing Brij97®:water ratios of 8:2 (w/w) (F8:2) and 7:3 (w/w) (F7:3), and one hexagonal phase in which the Brij97®:water ratio was 6:4 (w/w) (F6:4). As demonstrated in Fig. 2, the type of liquid crystalline phase was not altered by addition of MB at 0.1% (w/w), even though drug crystals were observed when water content decreased. An image of F6:4 is displayed in Fig. 2A, in which it is possible to observe

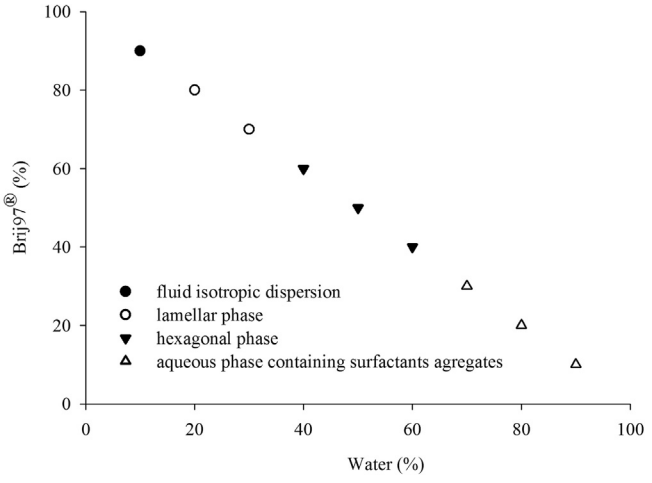

Fig. 1. Binary diagram resulting from the combination of Brij97®: water at different ratios.

the non-geometric and fan-like texture that characterizes the formation of hexagonal phase. Fig. 2B and C display isolated maltese crosses (F8:2) or assembled in strands (F7:3), indicating the formation of lamellar phase. In Fig. 2C it is possible to observe the presence of MB crystals in the F8:2 formulation.

3.2. Small angle X-ray scattering (SAXS) analysis

The small-angle X-ray scattering analysis was used to complement phase identification by polarized light microscopy. The analysis determines the scattering vector (q_{max}) as a function of the intensity at a maximum (I_{max}), and the correlation distance (d) between the objects can be determined ($d = 2\pi/q_{max}$). The ratio between the values of "d" allows identifying the liquid crystalline phase. According to the literature, the d1/d2 ratio equal to $\sqrt{4}$ refers to the periodicity of the lamellar phase; and the d1/d2 and d1/d3 ratios equal to $\sqrt{3}$ and $\sqrt{4}$, respectively, refer to the periodicity of the hexagonal phase (Calixto et al., 2016; Cintra et al., 2016; Rissi et al., 2014; Souza et al., 2014). The SAXS results (Fig. 3, Table 1) confirm that the F8:2 and F7:3 preparations follow the lamellar structural arrangement while the F6:4 preparation follows the hexagonal structural arrangement, and that the addition of MB at 0.1% (w/w) did not cause phase transformations (Table 1).

The lattice parameter provides more information regarding the internal structure of the liquid crystalline phase. The lattice parameter of the lamellar microstructure is represented by the distance between the bilayers, while the hexagonal microstructure is represented by the distance between the inner cores of the ordered micelles (Campos et al., 2012; Rossetti et al., 2011; Souza et al., 2014). The lattice parameter of the lamellar phases (F7:3 and F8:2) increased with the water content independently of the presence of MB (Table 1). MB incorporation (0.1%, w/w) in the system did not cause a significant change in the lattice parameter of the F6:4 hexagonal and F7:3 lamellar microstructure, but reduced the lattice parameter of the F8:2 lamellar microstructure.

In an attempt to maximize drug incorporation, the influence of MB at concentrations higher that 0.1% was also assessed. However, our results demonstrated that at 0.2%, MB altered the liquid crystalline structure of F6:4 and F7:3 (Fig. 4), with only F8:2 preserving its structure independent on MB concentration.

3.3. Rheology

The rheological profile of the selected liquid crystalline phases is shown in Fig. 5. Both the lamellar (F7:3 and F8:2) and hexagonal (F6:4) phases exhibited non-linear relationships between shear stress and shear rate, consistent with a non-Newtonian rheological behaviour. The decrease of viscosity with the progressive increase of the shear stress is consistent with pseudoplastic rheological behaviour, which is further supported by flow index values (obtained by Power law equation (Eq. (2))) varying from 0.220 to 0.269; a flow index lower than 1 indicates shear-thinning behaviour (Mahdi et al., 2011). F7:3 lamellar phase exhibited a slight increase of viscosity around 15–30 s^{-1}, similar to that observed by Hosmer et al. (2013), and it may be related to internal structure of the system.

F6:4 displayed higher viscosity throughout the analyzed range, as can be observed by the increased shear stress related to a specific value of shear rate. F7:3 displayed intermediate viscosity, followed by F8:2. To exemplify, at shear rate of 42 s^{-1}, the viscosity values of F6:4 (hexagonal phase), F7:3 and F8:2 (lamellar phases) were 32.03, 21.38 and 1.81 Pa.s, respectively; the control (3.0% HEC gel) displayed a viscosity of 7.8 Pa.s at the same rate of shear. These results demonstrate that increasing Brij97® concentration with a consequent reduction of water content progressively decreased the viscosity of the liquid crystalline phases.

By progressively reducing the shear stress, a hysteresis area was

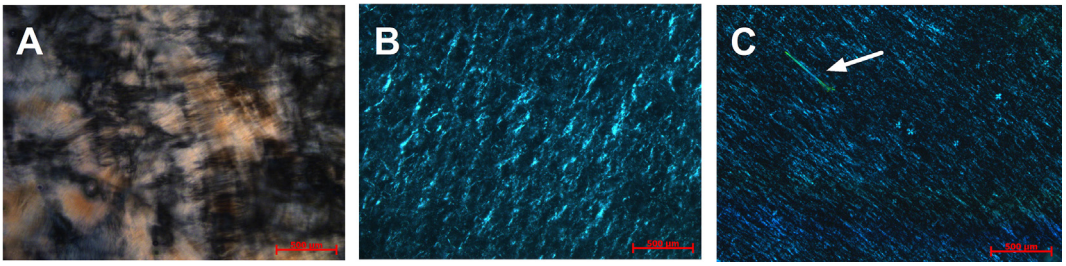

Fig. 2. Textures obtained under a polarized light microscope of the liquid crystalline phases resulting from the combination of Brij97® and water at different ratios, containing MB (0.1%, w/w). a) Brij97®:water at 6:4 (F6:4), b) Brij97®:water at 7:3 (F7:3), c) Brij97®:water at 8:2 (F8:2). The arrow in c) shows the presence of MB crystals.

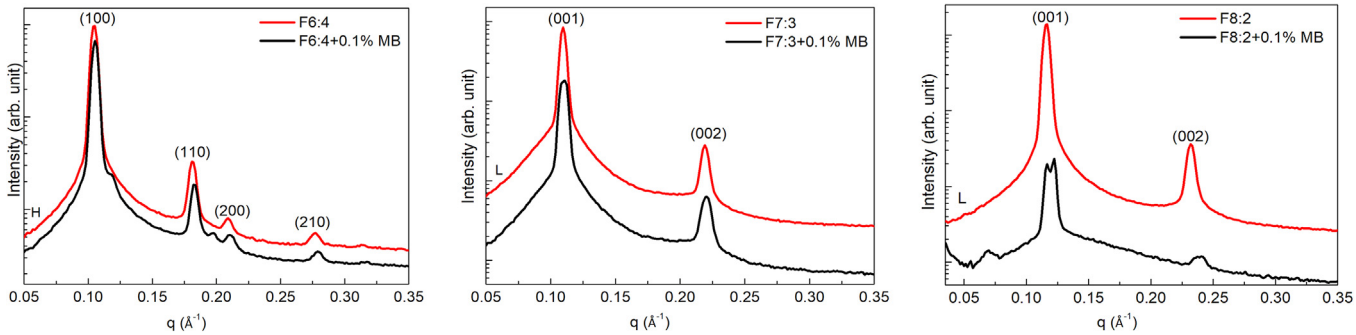

Fig. 3. SAXS patterns for liquid crystalline phases at Brij97®:water ratios of 8:2, 7:3 and 6:4, containing or not MB (0.1%, w/w). L = lamellar phase and H = hexagonal phase.

Table 1
Data obtained by SAXS from liquid crystalline phases containing or not MB (0.1%, w/w).

Samples	$d_{(hkl)}$ (nm) and *hkl*				ratio			$a_{(hkl)}$ (nm)				structure
	d1	d2	d3	d4	d1/d2	d1/d3	d1/d4	d1	d2	d3	d4	
F6:4	5.99(1 0 0)	3.47(1 1 0)	3.00(2 0 0)	2.27(2 1 0)	$\sqrt{3}$	$\sqrt{4}$	$\sqrt{7}$	6.91	6.90	6.92	6.87	Hex
F6:4 + MB (0.1%)	5.97(1 0 0)	3.45(1 1 0)	2.98(2 0 0)	2.25 (2 1 0)	$\sqrt{3}$	$\sqrt{4}$	$\sqrt{7}$	6.89	6.90	6.88	6.87	Hex
F7:3	5.72(0 0 1)	2.87(0 0 2)	–	–	$\sqrt{4}$	–	–	–	–	–	–	Lam
F7:3 + MB (0.1%)	5.66(0 0 1)	2.85(0 0 2)	–	–	$\sqrt{4}$	–	–	–	–	–	–	Lam
F8:2	5.39(0 0 1)	2.72(0 0 2)	–	–	$\sqrt{4}$	–	–	–	–	–	–	Lam
F8:2 + MB (0.1%)	5.14(0 0 1)	2.63(0 0 2)	–	–	$\sqrt{4}$	–	–	–	–	–	–	Lam

d = interplanar spacing; a = lattice parameter; hkl = Miller index, Hex = hexagonal, Lam = lamellar.

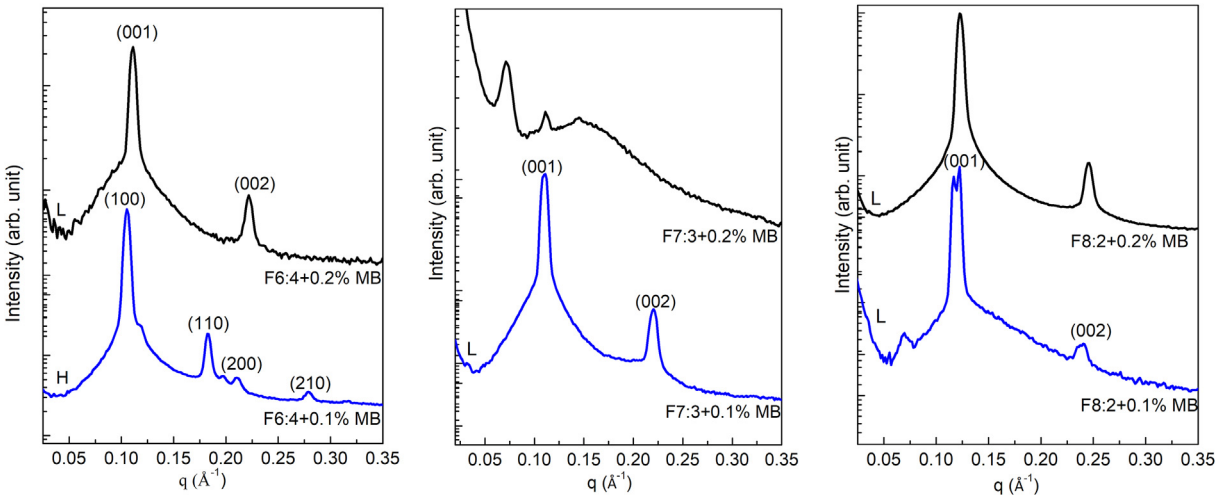

Fig. 4. SAXS patterns for liquid crystalline phases at Brij97®:water ratios of 8:2, 7:3 and 6:4, containing MB at different concentrations (0.1% and 0.2%, w/w). L = lamellar phase and H = hexagonal phase.

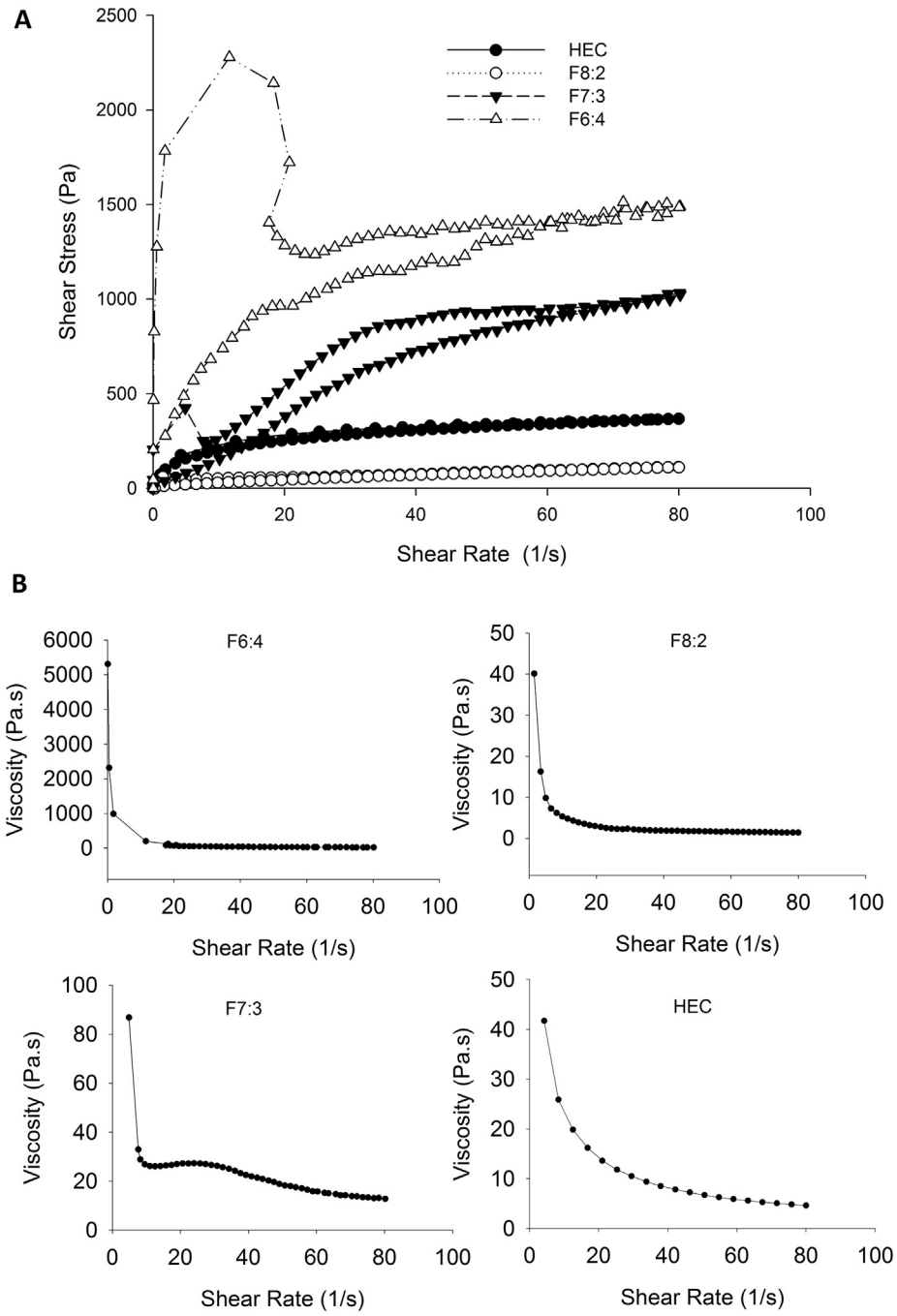

Fig. 5. A) Rheological behaviour of the liquid crystalline phases based on Brij97®:water at different ratios and the control (3.0% HEC gel). B) Apparent viscosity as function shear rate of the liquid crystalline phases based on Brij97®:water at different ratios and the control (3.0% HEC gel).

observed, indicating that a breakdown in the structure has occurred, and the systems require time to reorganize to their original state (thixotropy); this time is related to the degree of hysteresis (Aulton, 2007; Cintra et al., 2016). In other words, the larger the hysteresis area, the longer it takes for the system to restore to its original state. Similarly to the viscosity, hysteresis area differ among the liquid-crystalline systems; an increase of water content produces an increase of hysteresis area.

3.4. Stability study

Stability of the selected formulations containing 0.1% (w/w) of MB stored at room temperature and protected light was assessed for 9 months. Fig. 6 depicts variations in the MB content as a function of storage time, as well as the texture of the selected formulations observed under a polarized light microscope. As can be observed, the content of MB did not change significantly ($p > 0.05$) within the time period studied, and no changes on the type of liquid crystalline phase formed were observed, suggesting that the systems are stable at the studied conditions. The higher drug content (> 100%) during the stability study may be associated with the presence of drug crystals (F8:2) and the high viscosity of the systems (F6:4, F7:3 and F8:2), which might difficult the homogeneity of the drug in the system. Nevertheless, drug content was within the range 85.0%–115.0% (Chang et al., 2013), and content uniformity was achieved throughout the 9 months. The MB content was maintained for F8:2 system, in which MB crystals were

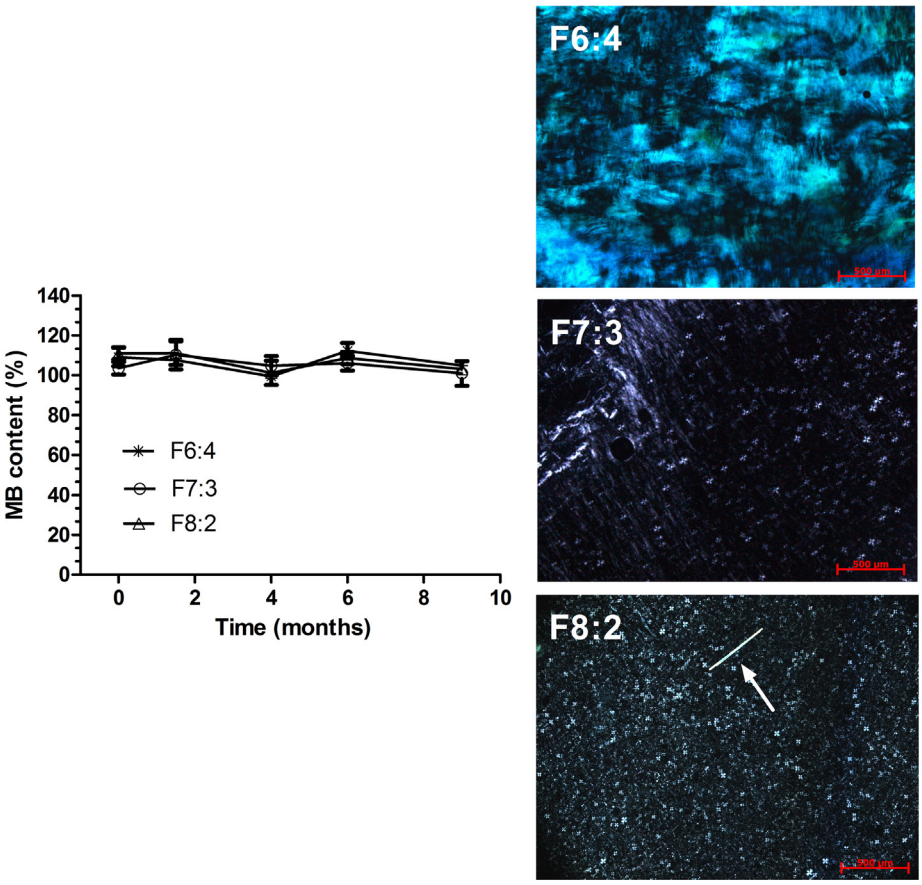

Fig. 6. Stability of the liquid crystalline phases and MB content as a function of time when stored at ambient temperature and protected from light. The initial MB concentration was 0.1%, w/w. Each point represents means ± standard deviation of 3 replicates. Representative textures of the formulations observed under a polarized light microscope after 9 months are displayed in the side panels. The arrow in F8:2 shows the presence of MB crystals.

present, suggesting that the viscosity of the system may have contributed to uniformity of content. The aspect of crystals did not change during the stability study.

3.5. In vitro release of MB

Release studies were carried out to evaluate the influence of the structure and composition of the liquid crystalline phase on the release of MB and, consequently, the amount of drug available to penetrate the skin. Compared to the control gel, MB release from all three liquid crystalline systems was significantly smaller ($p < 0.001$, Fig. 7A). At 6 h, the control gel released approximately 61% of MB, while formulations F8:2, F7:3 and F6:4 released approximately 12.2%, 6.1% and 10.7%, respectively. A comparison among the liquid crystalline phases at 6 h revealed that the amount of MB released from F8:2 was significantly higher compared to F7:3 (2.0-fold, $p < 0.01$) and that the amount of MB released from F6:4 was significantly higher compared to F7:3 (1.75-fold, $p < 0.05$) (Fig. 7B). To ensure that no phase transition occurred during the experiment, we also assessed formulation textures by polarized light microscopy. As can be observed in Fig. 7, the liquid crystalline texture was maintained throughout the experiment, suggesting that differences in drug release among the formulations should not to be attributed to alterations in their structure.

Kinetic analyses of the release profile showed a linear relationship between log of the amount remaining in the system versus time for F8:2, F7:3 and F6:4 ($r^2 = 0.999$, 0.978 and 0.986, respectively) (Fig. 7C), suggesting that drug release during the studied period follows first-order kinetics.

3.6. In vitro skin retention of MB

The amount of MB retained in the skin as a function of time is shown in Fig. 8. Using the control gel, the amount of MB retained at 3 and 6 h was 6.17 ± 1.16 μg/cm^2 and 7.43 ± 0.80 μg/cm^2, respectively. MB penetration increased using the liquid crystalline phases: at 3 h, an increase of 1.4- to 1.5-fold (8.92 ± 1.42 to 9.31 ± 1.55 μg/cm^2) was observed compared to the control, while increases of 1.3- to 2.1-fold (9.79 ± 1.22 to 15.70 ± 1.54 μg/cm^2) were observed at 6 h.

Comparing the liquid crystalline phases among each other, MB retention at 3 h was similar, but at 6 h, it was more pronounced using F8:2 (1.2- and 1.6-fold compared to F7:3 and F6:4, respectively) followed by F7:3 (1.3-fold higher than F6:4). The amount of MB permeated into the receptor phase was below the limit of quantification of the method (0.665 μg/mL), suggesting very low transdermal transport.

3.7. In vitro transepidermal water loss

The organization and chemical composition of the stratum corneum plays a fundamental role in the barrier function exerted by the skin. Changes in the physical or chemical structure of this barrier correlate with an increase in transepidermal water loss (TEWL), so this parameter was used to evaluate the barrier function of the skin after treatment with the selected formulations, and consequently, the influence of Brij97® concentration (Jiang et al., 2014; Pepe et al., 2013). The difference on ΔTEWL between control and HEC (3.0%, w/w) was not significant. Although we did not find significant differences among the liquid crystalline phases, they increased ΔTEWL compared to the control (water) or HEC (3.0%, w/w) by 2.0 to 2.8-fold (Fig. 9), with the lamellar phase F8:2 displaying the most pronounced effect (2.8-fold, $p < 0.001$). The least pronounced effect was observed for F6:4 (2.0-fold, $p < 0.05$), suggesting that Brij97® concentration, and consequently type of liquid crystalline phase, affects the barrier function of the skin.

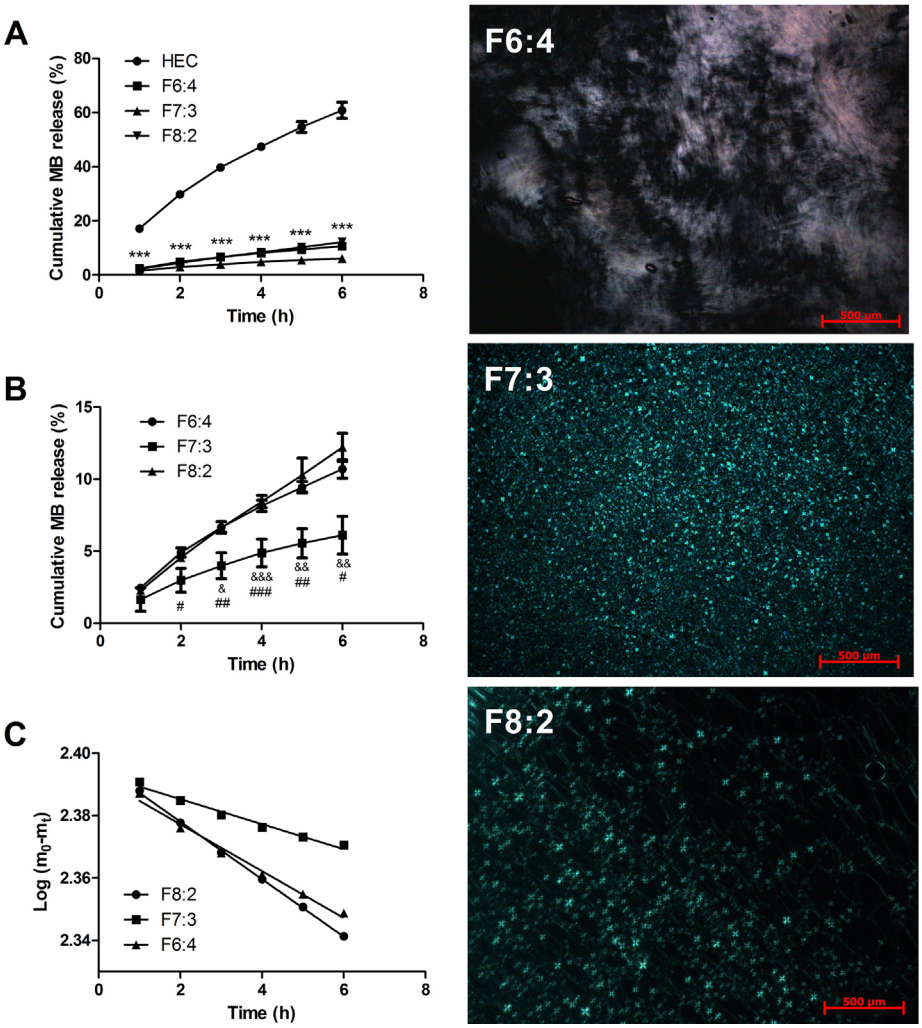

Fig. 7. *In vitro* release of MB. (A) Release profile of MB (0.1%, w/w) from liquid crystalline phases and control (HEC 3.0%, w/w); (B) Release profile of MB from liquid crystalline phases; $r^2 = 0.998$ for F8:2; $r^2 = 0.976$ for F7:3; $r^2 = 0.982$ for F6:4.; (C) fitting of the log of the amount remaining in the system as function of time (First-order model); $r^2 = 0.999$ for F8:2; $r^2 = 0.978$ for F7:3; $r^2 = 0.986$ for F6:4. Each point represents means ± standard deviation of 5–6 replicates. m_t is the amount of the MB released in time t, m_0 is the initial concentration of the MB. Textures obtained under a polarized light microscope of the liquid crystalline phases removed from the donor compartment after the 6-hour *in vitro* release study. One-way ANOVA – Tukey Kramer multiple comparisons test. $^{***}p < 0.001$, compared to the control (3.0% HEC gel), for its respective time. $^{\#\#\#}p < 0.001$, compared to F6:4, for its respective time; $^{\#\#}p < 0.01$, compared to F6:4, for its respective time; $^{\#}p < 0.05$, compared to F6:4, for its respective time. & $p < 0.05$, compared to F8:2, for its respective time; && $p < 0.01$, compared to F8:2, for its respective time; &&& $p < 0.001$, compared to F8:2, for its respective time.

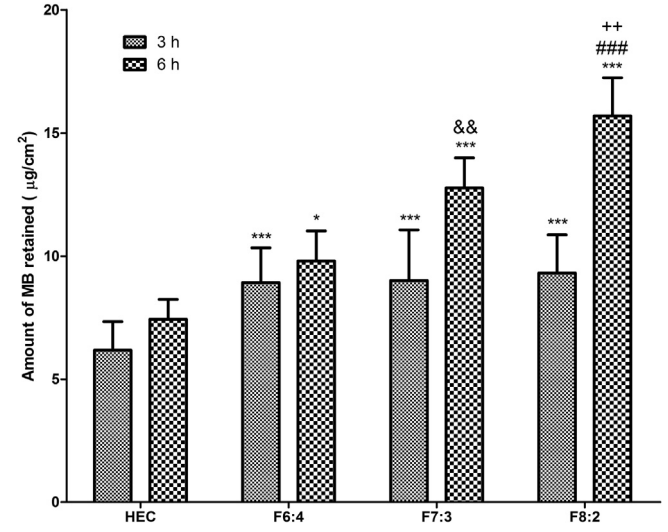

Fig. 8. Amount of MB retained in the skin at 3 or 6 h from liquid crystalline phases and control (3.0% HEC gel) containing 0.1% MB. Each point represents means ± standard deviation of 5–6 replicates. One-way ANOVA – Tukey Kramer multiple comparisons test. $^{***}p < 0.001$; $^{*}p < 0.05$, compared to the control (3.0% HEC gel), for their respective time. $^{\#\#\#}p < 0.001$, compared to F6: 4, for its respective time; $^{++}p < 0.01$, compared to F7:3, for its respective time; && $p < 0.01$, compared to F6:4, for its respective time.

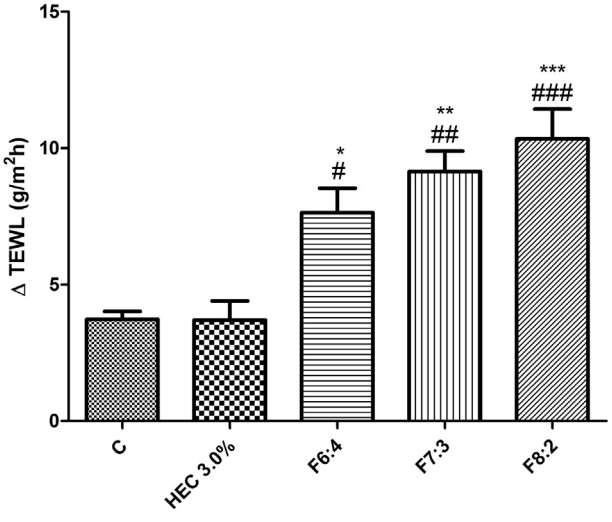

Fig. 9. Difference between transepidermal water loss values after treatment (6h) and before treatment (basal values) (ΔTEWL) with different formulations. Control (C) = the skin was exposed to water. Each point represents means ± standard deviation of 4–5 replicates. One-way ANOVA – Tukey Kramer multiple comparisons test. $^{\#\#\#}p < 0.001$, compared to Control; $^{\#\#}p < 0.01$, compared to Control; $^{\#}p < 0.05$, compared to Control; $^{***}p < 0.001$, compared to HEC; $^{**}p < 0.01$, compared to HEC; $^{*}p < 0.05$, compared to HEC.

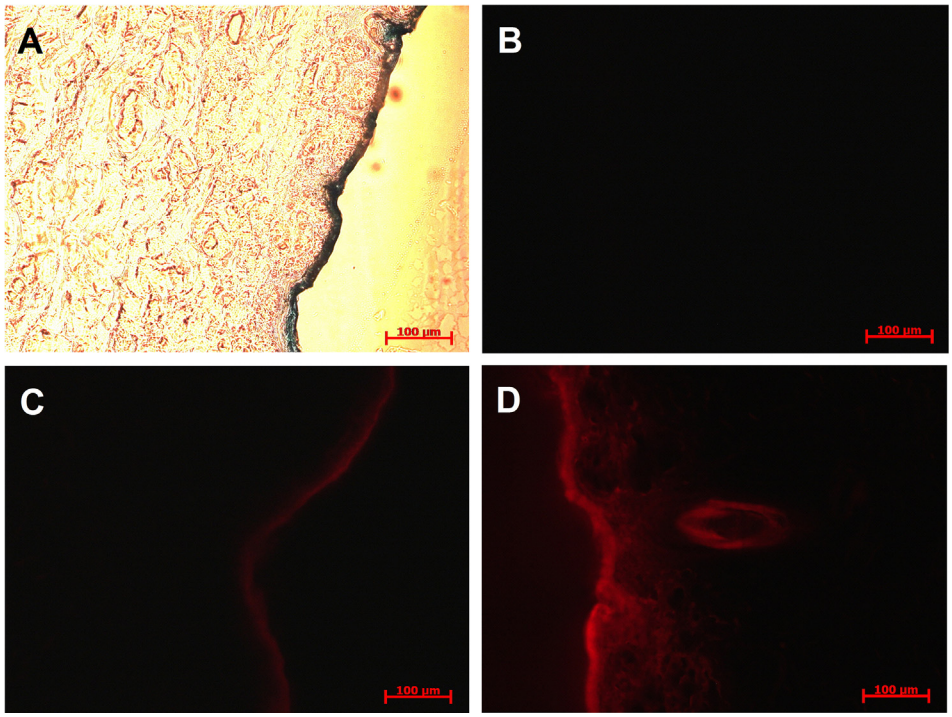

Fig. 10. Microscopic evaluation of porcine ear skin after treatment for 6 h with different formulations. (A) Light microscopy of skin treated with phosphate buffer (pH7.2, 0,1M). (B) Fluorescence microscopy of skin section treated with phosphate buffer (pH7.2, 0,1M). (C) Fluorescence microscopy of skin treated with the HEC 3.0% (w/w) containing MB (0.1%, w/w). (D) Fluorescence microscopy of skin treated with the F8:2 lamellar phase containing MB (0.1%, w/w). Sections were visualized using Rhodamine filter through a 20× objective. Three batches of each formulation were tested, and representative pictures are shown.

3.8. Fluorescence microscopy

The skin penetration of MB was visualized by fluorescence microscopy (Fig. 10). Untreated skin presented a very weak autofluorescence. When MB (0.1%, w/w) was incorporated in the HEC (3.0%, w/w) (control), fluorescence was predominantly present in the stratum corneum. On the other hand, treatment of the skin with the F8:2 lamellar phase containing MB (0.1%, w/w) resulted in a strong fluorescent staining of stratum corneum and viable epidermis. The staining was homogeneously distributed throughout the stratum corneum, suggesting MB penetration through this layer and not only through skin appendages.

3.9. Irritation potential

Hen's Egg Test – Chorioallantoic Membrane (HET-CAM) was originally developed to evaluate ocular irritation potential of substances, but it has been currently also used to evaluate skin irritation potential of formulations and their components, since they seem to have a good correlation (Mehling et al., 2007). The method is based on measurement of time dependent occurrence of effects on the chorioallantoic membrane when exposed to a test product (Scheel et al., 2011).

Representative pictures of the membranes after removal of the formulations were demonstrated in Fig. 11. Treatment with NaOH causes lysis, hemorrhage and coagulation within 5 min, resulting in a score of 16.9, which is consistent with its classification as irritant. Treatment with saline did not cause any alterations on the membranes. None of the formulations caused coagulation, while hemorrhage and few spots of lysis could be observed after treatment with F8:2 and F7:3, resulting in scores of 7.59 and 1.96, respectively, in accordance to the time in which they were first observed. The vascular reaction caused by F6:4 was milder, and was inconsistently observed in the eggs, leading to the lowest score (0.89) among the developed formulations, and its classification as slightly or not irritant.

4. Discussion

The present study assessed the influence of composition and internal structure of Brij97®-based liquid crystalline phases on the cutaneous delivery of MB. Brij97® is an amphiphilic molecule and has a non-polar (C18) monounsaturated (C9) alkyl chain coupled to the polar chain based on ethylene oxide (POE 10). When dispersed in aqueous solution, this molecule can be organized in different aggregates, as evidenced in the binary diagram (Fig. 1), in which isotropic, lamellar, hexagonal and aqueous micellar phases were successively formed with progressive addition of water in the system, similar to that observed by Kunieda et al. (1997).

The formed liquid crystalline structures can be justified by changes on the critical packaging parameter (CPP) of the molecule, which considers the hydrophobic chain volume (V), the headgroup area (Ao) and the hydrophobic chain length (L) of the molecule and is expressed by the following equation: CPP = V/Ao L (Israelachvili et al., 1976). In general, CPP values between 1/3 and 1/2 favors formation of cylindrical structures organized in hexagonal arrangements, while CPP values of ½-1 favor the arrangement in bilayers. According to the literature, Brij97® has a CPP value of 0.45, which favors the formation of cylindrical structures in hexagonal arrangement (Wang et al., 2005). The formation of the lamellar phase may be feasible with increasing Brij97® concentrations (and consequent water reduction) in the system, which causes the reduction of the area of the polar group (Ao), as consequence of the reduced water content, and of the overlap of chains from adjacent layers, leading an increased CPP (Wang et al., 2006).

Alterations in the lattice parameters indicate changes in the internal structure without phase transition. The lattice parameter of the lamellar microstructure increased with the water content in the system (F8:2 to F7:3), which resulted from hydration. The presence of other compounds and their concentration may induce phase transition (Rossetti et al., 2011), which can be attributed to their location in the polar or nonpolar domains of the system, and interference with the surfactant CPP, inducing phase transition (Hosmer et al., 2011; Souza et al., 2014). Additionally, the presence of hydrophilic molecules in the aqueous domain may also increase the polar group area of surfactant, contributing to the increase of the lattice parameter without necessarily causing phase transformation (Rossetti et al., 2011; Souza et al., 2014). According to polarized light microscopy and SAXS analysis, MB addition at 0.1% to F6:4, F7:3 and F8:2 did not induce phase transition, preclude

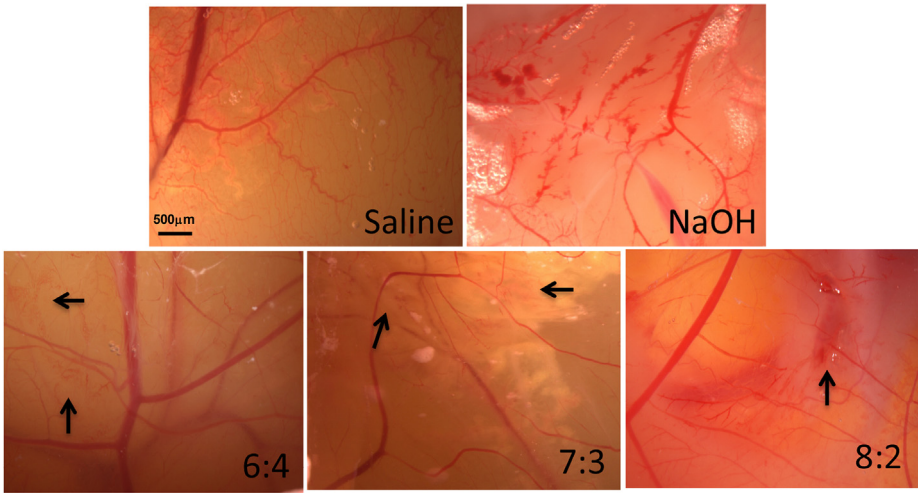

Fig. 11. Irritation potential assessed by HET-CAM. The arrows indicate regions where lysis or hemorrhage was noticed after treatment with the formulations for 5 min.

the formation of the liquid crystalline phases or change the lattice parameter of F6:4 hexagonal and F7:3 lamellar phases; however, it induced a reduction in the lattice parameter of F8:2. A similar effect has also been reported by Borgheti-Cardoso et al. (2016) and Souza et al. (2014), and attributed to dehydration of the aqueous domain of liquid crystalline system, as the hydrophilic molecules competes for water. SAXS studies also demonstrated that addition of MB at 0.2% in F6:4 induced phase transition, leading to formation of the lamellar phase. Phase transitions induced by drug concentration in Brij97®-based systems was also reported by Hosmer et al. (2011) as paclitaxel (a lipophilic drug) concentration increased (0.25%–0.5%, w/w). Because hydrophilic compounds like MB can compete for water, dehydration of the polar group and increase in the mobility of hydrocarbon chains are possible, resulting in alteration of CPP and phase transition (Rossetti et al., 2011; Souza et al., 2014). Based on these results, MB concentration of 0.1% was selected to allow a comparison of hexagonal and lamellar phases on its cutaneous delivery.

The rheological profile of the selected liquid crystalline phases is consistent with a thixotropic pseudoplastic rheological behaviour. Both viscosity and hysteresis area differ between the liquid-crystalline phases; an increase of water content produces an increase of viscosity and hysteresis area, suggesting that these parameters are related to the composition, structural organization and interaction forces between the components (Fujimura et al., 2016). The thixotropic pseudoplastic behaviour is an appropriate property for topical formulations: under the application of a force, the structure of the system tends to align in the direction of flow, reducing the resistance and facilitating the spreading of the system on the skin, whereas the systems gradually restructure, remaining at the target site, when the application force is removed (Aulton, 2007). This behaviour can be explained by the differences between the structural mobility of liquid crystalline phases. The lamellar phase is characterized by the formation of bilayers that are separated by water and this organization favors the sliding between the bilayers (Tyle, 1989) in the direction of the flow under the action of shear stress; while the hexagonal phase is characterized by the formation of cylinders that are arranged in hexagonal arrangement (Tyle, 1989), which may impose higher resistance to the flow, thus justifying the higher viscosity of F6:4

Results from release studies demonstrated that the liquid crystalline phases reduced the amount of MB released as a function of time compared to the control gel. While the higher viscosity of the F7:3 lamellar and F6:4 hexagonal phases may have contributed to this result, F8:2 is less viscous than the control gel, giving evidence that the structural organization of liquid crystalline constitute a barrier to MB release and impose drug diffusion restriction. As reported by Phelps et al (2011), the content of structure-forming surfactant affects the microstructure and viscosity of the system, and consequently drug diffusivity (Phelps et al., 2011). These results demonstrate the potential of both hexagonal and the lamellar phases to prolong MB release, but also that the composition and structure play an important role.

Brij97®/water partition coefficient of MB may have contributed to the higher MB release from F8:2 than F7:3. According to Carr et al. (1997), the partition coefficient of the drug between the Myverol™ and water interferes on drug release as a function of the increase in water content in the system. For a drug with a low Myverol™/water partition coefficient, an increase in the system aqueous content causes a reduction in drug concentration in the aqueous medium, which reduces drug release (Carr et al., 1997). The effect of drug partitioning between lipophilic and hydrophilic domains of the system has also been reported by Borgheti-Cardoso et al. (2016) using Vitamin E TPGS/isopropyl myristate/water for transdermal delivery of nicotine and Souza et al. (2014) using Myverol™/water for buccal delivery of poly(hexamethylene biguanide). Thus, it can be suggested that the low partitioning of MB, a hydrophilic drug, in the structural arrangement of the surfactant and the increase of the water content in the system can lead to a reduction of the MB concentration in the aqueous phase which reduces release. On the other hand, increasing Brij97®:water ratio increases MB concentration in the aqueous medium. In fact, the presence of MB crystals was observed in F8:2, suggesting water saturation and thus, high MB concentration in the aqueous phase. Considering that drug saturation increases thermodynamic activity, drug release and cutaneous penetration (Moser et al., 2001), we can infer that the lower aqueous content in F8:2 contributes to its efficacy and maximization of MB penetration (Carr et al., 1997; Otto et al., 2010, 2009).

The reason for the lower release from F7:3 is not clear. One possible explanation is that a small portion of the formulation underwent phase transition (at points of contact with the water-rich receptor phase); even though it was not overall perceptible by polarized light microscopy, this transition could have imposed a barrier for drug release as previously suggested by Farkas et al. (2000).

Independent of liquid crystalline phase, a linear relationship was found between log of the amount drug remaining in the system and time, indicative of first-order kinetics. This means that MB release from liquid crystalline phases followed a concentration gradient pattern, wherein the released amounts are related to the amounts remaining into the systems offering a sustained drug release. The kinetics obtained are in agreement with previous studies that evaluated ephedrine hydrochloride and glucose release from liquid crystalline phases (Makai

et al., 2003; Phan et al., 2011).

Even though MB release from the liquid crystalline phases was lower than the control gel, these systems were more effective at enhancing cutaneous delivery of MB, as demonstrated in MB skin retention studies and supported by fluorescence microscopy studies. This effect might be attributed to the interaction between the structure of the liquid crystalline phases and the lipid matrix of the stratum corneum, as well as to the effect of Brij97®, which has been described to favor the partitioning of the drug in the membrane and even induce fluidification of the stratum corneum lipid matrix, decreasing the barrier function of the tissue (Walters et al., 1988). In addition, the presence of hydrophilic domains in the liquid crystalline phase may hydrate corneocyte proteins and increase interlamellar volume of the lipid bilayer, leading to a disorganization of the stratum corneum barrier (Hosmer et al., 2011; Otto et al., 2010, 2009); stratum corneum hydration may also favor the partitioning of the hydrophilic drugs like MB (Otto et al., 2009).

Among the liquid crystalline phases studied, the F8:2 lamellar phase followed by F7:3 lamellar phase were more effective to improve cutaneous delivery of MB. The higher MB release from F8:2 may have contributed to the more pronounced MB retention compared to F7:3, but it cannot justify the superiority of F8:2 compared to F6:4, as both systems released similar amounts of MB. A possible explanation is the influence of viscosity on formulation spreading and contact with the skin. The higher fluidity of F8:2 and F7:3 lamellar phases might contribute to a more intimate contact and interaction of the formulations with the skin surface, favoring MB penetration. Another possible explication relates to structural arrangement of the system, because the lamellar structural arrangement of the system is similar to the arrangement of lipid matrix of stratum corneum and it may be responsible for the increase in drug penetration, as previously reported by Fonseca-Santos et al. (2017) and Muzzalupo et al. (2010). Additionally, the concentration of Brij97® affects cutaneous barrier function as demonstrated by increases in transepidermal water loss as the surfactant concentration increases. Compared with the control (water) and HEC (3.0%, w/w), the F8:2 lamellar phase showed a significant effect on TEWL ($p < 0.001$), followed by the F7:3 lamellar phase ($p < 0.01$) and F6:4 hexagonal phase ($p < 0.05$). However, this effect may have a limited importance, because no significant difference was found between the liquid crystalline phases.

Besides optimizing MB cutaneous delivery, F8:2 also increased irritation potential compared to control (saline). On the other hand, F7:3 and F6:4 were considered slightly or not irritating. The results are in agreement with Phelps et al. (2011), in which the increase of Brij®97 concentration increases cytotoxicity. Brij series surfactants are mild to moderately tolerated as classified by Draise score (Kapoor et al., 2009; Vian et al., 1995). It is recognized that surfactant monomers are capable of penetrating into the stratum corneum and inducing structural changes. The higher the critical micelle concentration of the surfactant, the greater the skin irritative potential, because the concentration of free monomers is higher. On the other hand, when the critical micelle concentration is achieved and nanostructured delivery systems are formed (as is the case of the present study), the irritant effect is reduced; however, if the critical micelle concentration is markedly exceeded, the irritation potential rises (Seweryn, 2018), which justifies the results obtained here. Therefore, F7:3 and F6:4 formulations may be better tolerated by the skin.

Different systems (solutions, liposome, niosome, microneedles, thermoresponsive polymer systems) have been suggested for the topical delivery of MB for PDT in the treatment of cutaneous diseases (Caffarel-Salvador et al., 2015; Fadel and Tawfik, 2014; Junqueira et al., 2016; Moftah et al., 2016; Samy et al., 2015); however, few studies consider *in vitro* skin permeation/retention studies, which makes it difficult to compare our results with previous reports. Junqueira et al. (2016) proposed the use of polymeric systems for MB release for PDT in the treatment of cutaneous infections caused by bacteria and fungi; within 24 h, amount of MB retained corresponded 0.38% of the total added dose (0.25% (w/w) of drug content in the system). In the present study, the amount of MB retained within 6 h using the liquid crystalline systems corresponded to 3.7–6.0%, using a lower drug content in the formulations (0.1%, w/w), clearly demonstrating the superiority of the liquid crystalline phases developed here. Therapeutic effectiveness studies are needed to obtain enough evidence for their potential use as delivery systems of MB in topical PDT.

5. Conclusion

The present study demonstrates that it is possible to increase the cutaneous delivery of MB using Brij97®-based liquid crystalline systems, and that this effect can be maximized as a function of the internal structure of the system, and water content, which optimizes the thermodynamic activity of the drug in the system, drug release, interaction and disruption of the cutaneous barrier function. Comparing the lamellar and hexagonal crystalline phases, higher cutaneous delivery of MB was obtained with the lamellar phase. Comparing the F8:2 and F7:3 lamellar phases, higher cutaneous delivery of MB was obtained with the F8:2 system. On the other hand, F7:3 and F6:4 phases might be better tolerated by the skin than F8:2.

These results show that a careful formulation design and characterization is essential to produce effective and safe systems for cutaneous delivery of MB.

Acknowledgments

The authors would like to thank Dr. Richardt Gama Landgraf for his permission to use polarized light microscope, as well as, “Coordenação de Aperfeiçoamento de Pessoal de Nível Superior” (CAPESP, Brazil), “Conselho Nacional de Desenvolvimento Científico e Tecnológico” (CNPq, Brazil, grant# 443549/2014-1) and “Fundação de Amparo à Pesquisa do Estado de São Paulo” (Fapesp, Brazil, grant# 2013/16617-7, grant# 2010/01404-0 and fellowship# 2017/23213-0). M.C.A. Fantini is researcher of CNPq.

Conflict of interest

The authors report no declarations of interest.

References

Aulton, M.E., 2007. Aulton’s Pharmaceutics. The Design and Manufacture of Medicines, third ed. Churchill Livingstone Elesevier, London.

Baran, T.M., Giesselman, B.R., Hu, R., Biel, M.A., Foster, T.H., 2010. Factors influencing tumor response to photodynamic therapy sensitized by intratumor administration of methylene blue. Laser Surg. Med. 42 (8), 728–735. https://doi.org/10.1002/lsm.20962.

Borgheti-Cardoso, L.N., de Vicentini, F.T.M. de C., Gratieri, T., Bentley, M.V.L.B., 2016. Liquid crystalline systems containing Vitamin E TPGS for the controlled transdermal nicotine delivery. Braz J Pharm Sci 52 (1), 191–200.

Brasil, 2003. Agência Nacional de Vigilância Sanitária. Guia para validação de métodos analíticos e bioanalíticos. Resolução RE no 899, 29 de maio de 2003. Diário Of. da União.

Caffarel-Salvador, E., Kearney, M.C., Mairs, R., Gallo, L., Stewart, S.A., Brady, A.J., Donnelly, R.F., 2015. Methylene blue-loaded dissolving microneedles: potential use in photodynamic antimicrobial chemotherapy of infected wounds. Pharmaceutics 7, 397–412. https://doi.org/10.3390/pharmaceutics7040397.

Calixto, G.M., Garcia, M.H., Cilli, E.M., Chiavacci, L.A., Chorilli, M., 2016. Design and characterization of a novel p1025 peptide-loaded liquid crystalline system for the treatment of dental caries. Molecules 21.

Campos, D.D.P. de, Cassu, S.N., Garcia, R.B.R., Queiroz, H.A.A. da S., Gonçalves, R.F.B., Kawachi, E.Y., 2012. Avaliação por SAXS e DSC das interações entre H2O e Renex-100. Quim Nov. 35, 355–359. https://doi.org/https://doi.org/10.1590/S0100-40422012000200023.

Carr, M.G., Corish, J., Corrigan, O.I., 1997. Drug delivery from a liquid crystalline base across visking and human stratum corneum. Int. J. Pharm. 157, 35–42. https://doi.org/10.1016/S0378-5173(97)00209-3.

Chang, R.-K., Raw, A., Lionberger, R., Yu, L., 2013. Generic development of topical dermatologic products: formulation development, process development, and testing of topical dermatologic products. AAPS J. 15, 41–52. https://doi.org/10.1208/s12248-012-9411-0.

Cintra, G.A., Pinto, L.A., Calixto, G.M., Soares, C.P., Von Zuben Ede, S., Scarpa, M.V.,

Gremiao, M.P., Chorilli, M., 2016. Bioadhesive surfactant systems for methotrexate skin delivery. Molecules 21, E231.
Fadel, M.A., Tawfik, A.A., 2014. New topical photodynamic therapy for treatment of hidradenitis suppurativa using methylene blue niosomal gel: a single-blind, randomized, comparative study. Clin. Exp. Dermatol. 40, 116–122. https://doi.org/10.1111/ced.12459.
Farkas, E., Zelkó, R., Németh, Z., Pálinkás, J., Marton, S., Rácz, I., 2000. The effect of liquid crystalline structure on chlorhexidine diacetate release. Int. J. Pharm. 193, 239–245. https://doi.org/10.1016/S0378-5173(99)00346-4.
Fonseca-Santos, B., Satake, C.Y., Calixto, G.M.F., Dos Ssantos, A.M., Chorilli, M., 2017. Trans-resveratrol-loaded nonionic lamellar liquid-crystalline systems: Structural, rheological, mechanical, textural, and bioadhesive characterization and evaluation of in vivo anti-inflammatory activity. Int. J. Nanomed. 12, 6883–6893. https://doi.org/10.2147/IJN.S138629.
Fujimura, A.T., Martinez, R.M., Pinho-Ribeiro, F.A., Dias, Lopes, da Silva, A.M., Baracat, M.M., Georgetti, S.R., Verri Jr., W.A., Chorilli, M., Casagrande, R., 2016. Resveratrol-loaded liquid-crystalline system inhibits UVB-induced skin inflammation and oxidative stress in mice. J. Nat. Prod. 27, 1329–1338. https://doi.org/10.1021/acs.jnatprod.5b01132.
Ganem-Quintanar, A., Quintanar-Guerrero, D., Buri, P., 2000. Monoolein: a review of the pharmaceutical applications. Drug Dev. Ind. Pharm. 26 (8), 809–820.
Guan, J., Lai, X., Wang, X., Leung, A.W., Zhang, H., Xu, C., 2014. Photodynamic action of methylene blue in osteosarcoma cells in vitro. Photodiagn. Photodyn. Ther. 11, 13–19. https://doi.org/10.1016/j.pdpdt.2013.09.003.
Hosmer, J.M., Shin, S.O.O.H., Nornoo, A., Zheng, H., Lopes, L.B., 2011. Influence of internal structure and composition of liquid crystalline phases on topical delivery of paclitaxel. J. Pharm. Sci. 100, 1444–1455. https://doi.org/10.1002/jps.
Hosmer, J.M., Steiner, A.A., Lopes, L.B., 2013. Lamellar liquid crystalline phases for cutaneous delivery of paclitaxel: impact of the monoglyceride. Pharm. Res. 30, 694–706. https://doi.org/10.1007/s11095-012-0908-0.
ICCVAM, 2010. ICCVAM Test Method Evaluation Report: Current Validation Status of In Vitro Test Methods Proposed for Identifying Eye Injury Hazard Potential of Chemicals and Products. NIH Publication No. 10-7553. Research Triangle Park, NC: National Institute of Environmental Health Sciences.
Israelachvili, J.N., Mitchell, D.J., Ninham, B.W., 1976. Theory of self-assembly of hydrocarbon amphiphiles into micelles and bilayers. J. Chem. Soc. Faraday Trans. 2 72, 1525–1568. https://doi.org/10.1039/F29767201525.
Jiang, J., Quan, P., Chen, Y., Fang, L., 2014. Mechanistic investigation and reversible effect of 2-isopropyl-5-methylcyclohexyl heptanoate on the in vitro percutaneous absorption of indomethacin. Drug Deliv. 21, 26–33. https://doi.org/10.3109/10717544.2013.840691.
Junqueira, M.V., Borghi-Pangoni, F.B., Ferreira, S.B.S., Rabello, B.R., Hioka, N., Bruschi, M.L., 2016. Functional polymeric systems as delivery vehicles for methylene blue in photodynamic therapy. Langmuir 32, 19–27. https://doi.org/10.1021/acs.langmuir.5b02039.
Kapoor, Y., Howell, B.A., Chauhan, A., 2009. Liposome assay for evaluating ocular toxicity of surfactants. Invest. Ophthal. Vis. Sci. 50, 2727–2735. https://doi.org/10.1167/iovs.08-2980.
Kunieda, H., Shigeta, K., Ozawa, K., Suzuki, M., 1997. Self-organizing structures in poly (oxyethylene) oleyl ether-water system. J. Phys. Chem. B 101, 7952–7957. https://doi.org/10.1021/jp9713322.
Mahdi, E.S., Noor, A.M., Sakeena, M.H., Abdullah, G.Z., Abdulkarim, M.F., Sattar, M.A., 2011. Formulation and in vitro release evaluation of newly synthesized palm kernel oil esters-based nanoemulsion delivery system for 30% ethanolic dried extract derived from local Phyllanthus urinaria for skin antiaging. Int. J. Nanomed. 6, 2499–2512. https://doi.org/10.2147/ijn.s22337.
Makai, M., Csányi, E., Németh, Z., Pálinkás, J., Eros, I., 2003. Structure and drug release of lamellar liquid crystals containing glycerol. Int. J. Pharm. 256, 95–107. https://doi.org/10.1016/S0378-5173(03)00066-8.
Mehling, A., Kleber, M., Hensen, H., 2007. Comparative studies on the ocular and dermal irritation potential of surfactants. Food Chem. Toxicol. 45, 747–758. https://doi.org/10.1016/j.fct.2006.10.024.
Moftah, N.H., Ibrahim, S.M., Wahba, N.H., 2016. Intense pulsed light versus photodynamic therapy using liposomal methylene blue gel for the treatment of truncal acne vulgaris: a comparative randomized split body study. Arch. Dermatol. Res. 308, 263–268. https://doi.org/10.1007/s00403-016-1639-6.
Moser, K., Kriwet, K., Naik, A., Kalia, Y.N., Guy, R.H., 2001. Passive skin penetration enhancement and its quantification in vitro. Eur. J. Pharm. Biopharm. 52, 103–112.
Muzzalupo, R., Tavano, L., Nicoletta, F.P., Trombino, S., Cassano, R., Picci, N., 2010. Liquid crystalline pluronic 105 pharmacogels as drug delivery systems: Preparation, characterization, and in vitro transdermal release. J. Drug Target. 18, 404–411. https://doi.org/10.3109/10611860903494211.
Orth, K., Beck, G., Genze, F., Ruck, A., 2000. Methylene blue mediated photodynamic therapy in experimental colorectal tumors in mice. J. Photochem. Photobiol. B Biol. 57, 186–192. https://doi.org/https://doi.org/10.1016/S1011-1344(00)00105-6.
Orth, K., Russ, D., Beck, G., Ruck, A., Beger, H.G., 1998. Photochemotherapy of experimental colonic tumours with intra-tumorally applied methylene blue. Langenbecks Arch Surg. 383, 276–281.
Otto, A., Du Plessis, J., Wiechers, J.W., 2009. Formulation effects of topical emulsions on transdermal and dermal delivery. Int. J. Cosmet. Sci. 31, 1–19. https://doi.org/10.1111/j.1468-2494.2008.00467.x.
Otto, A., Wiechers, J.W., Kelly, C.L., Dederen, J.C., Hadgraft, J., Du Plessis, J., 2010. Effect of emulsifiers and their liquid crystalline structures in emulsions on dermal and transdermal delivery of hydroquinone, salicylic acid and octadecenedioic acid. Ski. Pharmacol. Physiol. 21, 273–282.
Park, E.S., Chang, S.Y., Hahn, M., Chi, S.C., 2000. Enhancing effect of polyoxyethylene alkyl ethers on the skin permeation of ibuprofen. Int. J. Pharm. 209, 109–119. https://doi.org/10.1016/S0378-5173(00)00559-7.
Pepe, D., McCall, M., Zheng, H., Lopes, L.B., 2013. Protein transduction domain-containing microemulsions as cutaneous delivery systems for an anticancer agent. J. Pharm. Sci. 102, 1476–1487. https://doi.org/10.1002/jps.23482.
Phan, S., Fong, W.K., Kirby, N., Hanley, T., Boyd, B.J., 2011. Evaluating the link between self-assembled mesophase structure and drug release. Int. J. Pharm. 421, 176–182. https://doi.org/10.1016/j.ijpharm.2011.09.022.
Phelps, J., Bentley, M.V.L.B., Lopes, L.B., 2011. In situ gelling hexagonal phases for sustained release of an anti-addiction drug. Colloids Surf B Biointerfaces 87, 391–398. https://doi.org/10.1016/j.colsurfb.2011.05.048.
Rissi, N.C., Guglielmi, D.A.S., Corrêa, M.A., Chiavacci, L.A., 2014. Relationship between composition and organizational levels of nanostructured systems formed by Oleth 10 and PPG-5-Ceteth-20 for potential drug delivery. Braz. J. Pharm. Sci. 50, 653–661. https://doi.org/https://doi.org/10.1590/S1984-82502014000300025.
Rossetti, F.C., Fantini, M.C., Carollo, A.R.H., Tedesco Bentley, A.C.M.V.L., 2011. Analysis of liquid crystalline nanoparticles by small angle X-ray diffraction: evaluation of drug and pharmaceutical additives influence on the internal structure. J. Pharm. Sci. 100, 2849–2857. https://doi.org/10.1002/jps.22522.
Samy, N.A., Salah, M.M., Ali, M.F., Sadek, A.M., 2015. Effect of methylene blue-mediated photodynamic therapy for treatment of basal cell carcinoma. Laser Med. Sci. 30, 109–115. https://doi.org/10.1007/s10103-014-1609-1.
Scheel, J., Kleber, M., Kreutz, J., Lehringer, E., Mehling, A., Reisinger, K., Steiling, W., 2011. Eye irritation potential: usefulness of the HET-CAM under the globally harmonized system of classification and labeling of chemicals (GHS). Regul. Toxicol. Pharm. 59, 471–492. https://doi.org/10.1016/j.yrtph.2011.02.003.
Seong, D., Kim, Y., 2015. Enhanced photodynamic therapy efficacy of methylene blue-loaded calcium phosphate nanoparticles. J. Photochem. Photobiol. B Biol. 146, 34–43. https://doi.org/10.1016/j.jphotobiol.2015.02.022.
Seweryn, A., 2018. Interactions between surfactants and the skin – theory and practice. Adv Colloid Interf Sci #pagerange#. doi:10.1016/j.cis.2018.04.002.
Souza, C., Watanabe, E., Borgheti-Cardoso, L.N., De Abreu Fantini, M.C., Lara, M.G., 2014. Mucoadhesive system formed by liquid crystals for buccal administration of poly(hexamethylene biguanide) hydrochloride. J. Pharm. Sci. 103, 3914–3923.
Tardivo, J.P., Del Giglio, A., De Oliveira, C.S., Gabrielli, D.S., Junqueira, H.C., Tada, D.B., Severino, D., De Fátima Turchiello, R., Baptista, M.S., 2005. Methylene blue in photodynamic therapy: From basic mechanisms to clinical applications. Photodiagn. Photodyn. Ther. 2, 175–191. https://doi.org/10.1016/S1572-1000(05)00097-9.
Tardivo, J.P., Del Giglio, A., Paschoal, L.H.C., Ito, A.S., Baptista, M.S., 2004. Treatment of melanoma lesions using methylene blue and RL50 light source. Photodiagn. Photodyn. Ther. 1, 345–346. https://doi.org/10.1016/S1572-1000(05)00005-0.
Thomas, S., Vieira, C.S., Hass, M.A., Lopes, L.B., 2014. Stability, cutaneous delivery, and antioxidant potential of a lipoic acid and alpha-tocopherol codrug incorporated in microemulsions. J. Pharm. Sci. 103, 2530–2538. https://doi.org/10.1002/jps.24053.
Tyle, P., 1989. Liquid Crystal and Their Application in Drug Delivery, Controlled Released of Drug: Polymers and Aggregate Systems. Morton Rosoff UHC Publisher, New York.
Vian, L., Vincent, J., Maurin, J., Fabre, I., Giroux, J., 1995. Comparison of three in vdro cytotoxicity assays for estimating surfactant ocular irritation. Toxic. Vitr. 9, 185–190.
Walker, I., Gorman, S.A., Cox, R.D., Vernon, D.I., Brown, S.B., 2004. A comparative analysis of phenothiazinium salts for the photosensitisation of murine fi brosarcoma (RIF-1) cells in vitro. Photochem. Photobiol. Sci. 3, 653–659. https://doi.org/10.1039/b400083h.
Walters, K.A., Walker, M., Olejnik, O., 1988. Non ionic surfactant effects on hairless mouse skin permeability characteristics. J. Pharm. Pharmacol. 40, 525–529.
Wang, Z., Diao, Z., Liu, F., Li, G., Zhang, G., 2006. Microstructure and rheological properties of liquid crystallines formed in Brij 97/water/IPM system. J. Colloid Interface Sci. 297, 813–818. https://doi.org/10.1016/j.jcis.2005.11.021.
Wang, Z., Liu, F., Gao, Y., Zhuang, W., Xu, L., Han, B., Li, G., Zhang, G., 2005. Hexagonal liquid crystalline phases formed in ternary systems of Brij 97 – water – ionic liquids. Langmuir 21, 4931–4937.
Yu, J., Hsu, C., Huang, C., Chang, P., 2014. Development of therapeutic au − methylene blue nanoparticles for targeted photodynamic therapy of cervical cancer cells. ACS Appl. Mater. Interfaces 7, 432–441. https://doi.org/10.1021/am5064298.